TISSUE ENGINEERING: Part A
Volume 15, Number 3, 2009

DOI: 10.1089/ten.tea.2008.0051

Engineering Endochondral Bone: *In Vitro* Studies

Serafim M. Oliveira, M.S.,[1–4] Isabel F. Amaral, Ph.D.,[2]
Mário A. Barbosa, Ph.D.,[2,3] and Cristina C. Teixeira, D.M.D., M.S., Ph.D.[4]

Chitosan scaffolds have been shown to possess biological and mechanical properties suitable for tissue engineering and clinical applications. In the present work, chitosan sponges were evaluated regarding their ability to support cartilage cell proliferation and maturation, which are the first steps in endochondral bone formation. Chitosan sponges were seeded with chondrocytes isolated from chicken embryo sterna. Chondrocyte/chitosan constructs were cultured for 20 days, and treated with retinoic acid (RA) to induce chondrocyte maturation and matrix synthesis. At different time points, samples were collected for microscopic, histological, biochemical, and mechanical analyses. Results show chondrocyte attachment, proliferation, and abundant matrix synthesis, completely obliterating the pores of the sponges. RA treatment caused chondrocyte hypertrophy, characterized by the presence of type X collagen in the extracellular matrix and increased alkaline phosphatase activity. In addition, hypertrophy markedly changed the mechanical properties of the chondrocyte/chitosan constructs. In conclusion, we have developed chitosan sponges with adequate pore structure and mechanical properties to serve as a support for hypertrophic chondrocytes. In parallel studies, we have evaluated the ability of this mature cartilage scaffold to induce endochondral ossification.

Introduction

Bone is an important component of the musculoskeletal system and often suffers injuries (caused by trauma, tumors, and others pathologies) that may result in considerable tissue loss. To address these problems, different materials, inert or bioactive, have been used for bone replacement or regeneration. Some of these materials are metals[1–3] and ceramics.[4–6] More recently, synthetic polymers[7–10] and natural polymers[11,12] have been used as templates for bone growth and regeneration.

Chitosan, the product of the partial deacetylation of the naturally occurring polysaccharide, chitin, has been shown to possess biological and mechanical properties suitable for clinical applications.[13–15] It is reported to be biocompatible and biodegradable in the presence of lysozyme, and its degradation products are nontoxic and can be incorporated into the extracellular matrix for rebuilding of normal tissues.[16–20] These properties, together with the ability to promote bone cell growth and differentiation, have stimulated the use of chitosan as a bone regeneration template.[14,21] Moreover, its structural similarity to various glycosaminoglycans and hyaluronic acid present in articular cartilage makes chitosan one of the most suitable materials for cartilage regeneration applications.[17,22,23] Indeed, chondrocytes have been successfully cultured on chitosan, and *in vivo* studies showed good results when this material was used as an articular cartilage implant.[22,24,25]

Although chitosan has been used as a scaffold for articular cartilage and bone formation by direct differentiation of mesenchymal cells into chondrocytes and osteoblast, respectively, to the best of our knowledge, it has not been used as a template for endochondral ossification. The endochondral ossification pathway involves an intermediate cartilage stage and is responsible for the formation of long bones, vertebra, and the cranial base during development. During bone elongation, endochondral ossification mediates growth via the activity of cells in the growth plates. The growth plates are discs of transient cartilage (not permanent cartilage as in the articular surface), located at the end of long bones. Within the growth plates, chondrocytes undergo maturation/hypertrophy coordinating the replacement of the calcified cartilage matrix by new bone.

The goal of the present work was to investigate chitosan's capability to support growth cartilage cell proliferation and maturation, as well as its potential as a template for endochondral ossification. There are numerous advantages in the use of the endochondral pathway for bone tissue engineering.

[1]Department of Mechanical Engineering, ESTV—Escola Superior de Tecnologia de Viseu, Viseu, Portugal.
[2]Divisão de Biomateriais, INEB—Instituto de Engenharia Biomédica, Porto, Portugal.
[3]Department of Metallurgy and Materials, FEUP—Faculdade de Engenharia da Universidade do Porto, Porto, Portugal.
[4]Department of Basic Science and Craniofacial Biology, New York University College of Dentistry, New York, New York.

Chondrocytes are resistant to low oxygen levels[26] and can induce vascular invasion and osteogenesis,[27,28] therefore allowing the creation of larger osteoinductive templates. Upon implantation, this template could behave like a growth plate, remodeling into the required bone, mimicking the natural process of endochondral ossification. In fact, a major problem in engineering articular cartilage is the tendency of the cells to undergo further maturation.[29–32] We sought to take advantage of this pathway for bone regeneration.

Materials and Methods

Preparation and characterization of chitosan powder and 3D scaffolds

Squid pen chitosan (Chitosan 123) was kindly supplied by France Chitine (Orange, France). After a purification step, chitosan with a degree of acetylation (DA) of ≅ 4% was prepared by heterogeneous deacetylation, according to Amaral *et al.*[33] The physicochemical properties of the resultant chitosan in terms of DA, weight average molecular weight (M_w), polydispersity index (PDI), and intrinsic viscosity ([η]) are presented in Table 1. The DA was determined by Fourier transform infrared (FT-IR), while the M_w, M_n, PDI, and [η] were determined by high-performance size-exclusion chromatography.[33] Three-dimensional (3D) porous scaffolds were prepared from 2% (w/v) chitosan acidic solutions via thermally induced phase separation and subsequent sublimation of the ice crystals. Briefly, chitosan solution was poured onto 24-well tissue culture polystyrene plates (800 μL/well), frozen at −20°C, and subsequently lyophilized during 48 h. The resultant planar sponges were cut into $4\times4\times1\,mm^3$ pieces, immersed in absolute ethanol, hydrated in serial diluted ethanol solutions, and finally equilibrated in Hank's balanced salt solution (HBSS) (Gibco, Carlsbad, CA).

Scanning electronic microscopy

Average pore diameter was measured on cross sections of scanning electronic microscopy (SEM) images. The maximum (l) and minimum (h) pore lengths were measured using a Cell Observer System (Carl Zeiss, Goettingen, Germany), and the average diameter was determined using the following equation: $d = \sqrt{l \cdot h}$. Results are the average (±SD) of 20 measurements.

Cell morphology, attachment, and proliferation were also assessed by SEM. Briefly, the samples were collected and fixed with 2% glutaraldehyde for 5 min at 37°C, followed by 1 h incubation at room temperature (RT) and overnight incubation at 4°C. Samples were dehydrated in serial ethanol solutions, and critical-point dried. Finally, scaffolds were cut, glued on steel stubs, coated with gold-palladium, and analyzed on both top and cross-sectional areas by SEM.

Table 1. Chitosan Powder Properties

DA (%)	*M_w ($\times10^5$) (Da)*	*PDI*	*[η] (dL/g)*
4.23 ± 0.46	2.1 ± 0.1	2.1 ± 0.2	8.20 ± 0.29

DA, degree of acetylation; M_w, weight average molecular weight; PDI, polydispersity index = (M_w/M_n); [η], intrinsic viscosity.

Mechanical properties tests

Creep and load deformation tests were performed on sponges cultured with chondrocytes, sponges without cells, as well as on tibia growth plates from 6-week-old chickens. For the creep test, samples were frozen in liquid nitrogen. The test was carried out on samples confined to a chamber in a bath of media, and loaded using a porous indenter (EnduraTEC-ELF 3200; Minnetonka, MN). Samples were rapidly loaded to 10 g, then the load held constant, and the change in displacement monitored for 1200 s. Strain versus time curves were analyzed using the biphasic theory of Mow *et al.*,[34] and the aggregate modulus and permeability computed. The load deformation test was performed on samples with 5 mm diameter, loaded with a flat, nonporous plate (EnduraTEC-ELF 3200). A load of 15 g was applied (47% strain produced). The stress versus strain plot was fitted with an exponential curve, and the slope at 30% strain computed as the elastic modulus.

Chondrocytes culture

Cephalic (CP) and caudal (CD) chondrocytes were isolated from the upper and lower region of sternum of 14-day chicken embryos, according to the method described by Iwamoto *et al.*[35] Chondrocytes were allowed to proliferate in 100 mm dishes for 7 days at 37°C and 5% CO_2 in Dulbecco's modified high-glucose Eagle's medium (DMEM) containing 10% NU Serum and 100 U/mL of penicillin/streptomycin (Fisher Scientific, Fairlawn, NJ). After cell expansion, 200,000 cells (15 μL of cell suspension) were seeded into the hydrated sponges previously placed in a 96-well plate. Culture medium was added 2 h after cell seeding and changed daily for 20 days. Cultures also received 400 U/mL of hyaluronidase and ascorbic acid (10–50 μg/mL). After 10 days, cultures were treated daily (for another 10 days) with 100 nM all-trans retinoic acid (RA) to induce chondrocyte maturation and matrix synthesis. CD chondrocytes do not respond to RA treatment, represent a permanent cartilage phenotype, and thus were used as control. Samples were collected every 5 days and used for different analysis. All chemicals, unless otherwise stated, were obtained from Sigma-Aldrich (St Louis, MO).

Cell solubilization

Three sets of two sponges for both CP and CD chondrocytes were collected, washed with phosphate buffered saline, immersed in 150 μL of 0.1% Triton×100 (Fisher Scientific), crushed manually, and centrifuged at 850 g for 3 min. The supernatant was used for measurement of alkaline phosphatase (AP) activity and protein and DNA content.

Protein and DNA analyses

Protein content was determined using a DC protein assay (BioRad Laboratories, Hercules, CA), according to the manufacturer's protocol, and absorbance measured at 750 nm using bovine serum albumin as standard. Total DNA amount was measured according to the procedure described by Teixeira *et al.*[36] using a bisBenzididazole dye (Hoechst 33258 dye; Polyscience, Northampton, UK). Fluorescence was measured at 365 nm excitation and 460 nm emission wavelengths. The results were extrapolated from a standard curve using salmon testis DNA (Sigma-Aldrich).

Alkaline phosphatase activity

For measurement of AP activity, samples were mixed with a fresh solution of 1 volume of 1.5 M tris-HCl pH 9.0 containing 7.5 mM *p*-nitrophenylphosphate, 1 mM $ZnCl_2$, and 1 mM $MgCl_2$. Changes in absorbance were measured spectrophotometrically at 410 nm for 10 min; changes over time correspond to the *p*-nitrophenylphosphate hydrolysis to *p*-nitrophenol. AP activity was expressed as nmol of product/min/mg of protein; 1 absorbance unit change corresponds to 64 nmol of product.

RNA isolation and real-time reverse transcriptase–polymerase chain reaction

RNA was isolated before the first day of RA treatment (day 10) and 10 days after RA treatment (day 20). Total RNA was extracted with Trizol® reagent (Life Technologies, Gaithersburg, MD) according to the manufacturer's instructions with some modifications. Briefly, samples were frozen in liquid nitrogen and crushed, Trizol reagent was added, and the samples were vortexed for 30 s and then kept at 4°C for 2 h. Phase separation was achieved by adding chloroform (0.2 volumes) to the mixture for 15 min and then centrifuging it at 12,000 *g* for 30 min at 4°C. The upper aqueous phase containing the RNA was collected, mixed with a high salt precipitation solution (0.8 M sodium citrate and 1.2 M NaCl and isopropanol), and centrifuged at maximum speed for 30 min at 4°C. RNA purification was completed using RNA micro kit (Qiagen, Chatsworth, CA) according to the RNeasy cleanup protocol. Real-time reverse transcriptase–polymerase chain reaction (RT-PCR) was performed using QuantiTect SYBR Green RT-PCR kit (Qiagen), a DNA Engine Optican2 system (Roche Molecular Systems, Pleasanton, CA), and primers specific for the following chick genes: *type X collagen* (forward: AGTGC TGTCATTGATCTCATTGGA; reverse: TCAGAGGAATAGA GACCATTGGATT), *AP* (forward: CCTGACATCGAGGTG ATCCT; reverse: GAGACCCAGCAGGAAGTCCA), *type I collagen* (forward: GCCGTGACCTCAGACTTAGC; reverse: TTTTGTCCTTGGGGTTCTTG), *runx2* (forward: CTTAGG AGAAGTGCCCGATG; reverse: CCATCCACCGTCACCTT TAT), and *VEGF* (forward: GGAAGCCCAACGAAGTTATC; reverse: AACCCGCACATCTCATCAG). *Acidic ribosomal protein (RP)* mRNA was used as a reference for quantification (forward: AACATGTTGAACATCTCCCC; reverse: ATCTGC AGACAGACGCTGGC). All primers were purchased from Qiagen (Valencia, CA). Relative transcript levels were presented as fold change in gene expression and calculated using the threshold cycle (Ct) and the formula below, where CD refers to CD chondrocytes, CP refers to CP chondrocytes, and RP refers to the acidic ribosomal protein: $x = 2^{\Delta\Delta Ct}$, in which $\Delta\Delta Ct = \Delta E - \Delta C$, and $\Delta E = CtCP - CtRP$, and $\Delta C = CtCD - CtRP$. A $\Delta\Delta Ct < 0$ was considered a decrease, while a $\Delta\Delta Ct > 0$ was considered an increase in gene expression.

Histology and immunohistochemistry

Scaffolds were collected, fixed in 10% phosphate buffered formalin, dehydrated in alcohol series, and embedded in paraffin, and 5-μm-thick sections were cut and stained with hematoxylin and eosin (H&E). For immunohistochemistry, sections were deparaffinized, rehydrated, and immunostaining performed using antibodies specific for chick *type X collagen* with the Vectastain ABC kit (Vector Laboratories, Burlingame, CA) according to the manufacturer's instructions. Sections were counter stained with 1% alcian blue and light green. The stained sections were mounted under glass coverslips, and scanned on Scan Scope GL series optical microscope (Aperio, Bristol, UK) at 20× magnification.

Statistical analysis

All experiments were repeated three to four times, and the mean and standard error of the mean were determined. Significant differences were assessed by ANOVA. A *p*-value refers to a comparison of a measured parameter in the experimental group with that of the appropriate control; significance was set at $p < 0.05$.

Results

Characterization of chitosan scaffolds

Images obtained by SEM (Fig. 1) of cross sections of sponges show a homogeneous pore size and distribution. At higher magnification (500×) the interconnectivity can be observed among pores with an average pore size of 92 ± 12 μm (Fig. 1B). This pore dimension is considered to be within the desired range for tissue engineering applications.[37,38]

Mechanical properties

The compression strength, elastic modulus, aggregate modulus, and permeability of chitosan scaffolds while altered in the presence of cells did not approach the properties of chick growth plates (Table 2). Both chondrocytes/chitosan

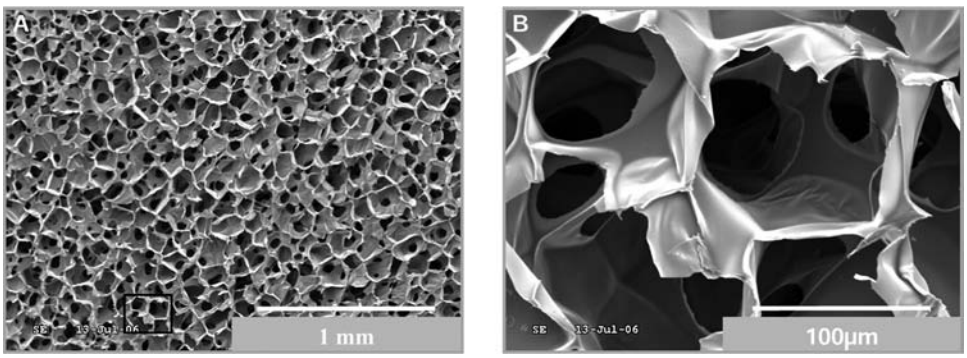

FIG. 1. Homogeneous distribution of pores in chitosan sponges. SEM photomicrographs of cross sections of dehydrated chitosan sponges. Image (**A**) (lower magnification) shows high homogeneity in the size and distribution of pores, and image (**B**) (higher magnification) shows the interconnectivity.

Table 2. Properties of Scaffolds

	D (μm)	*σ (kPa)*	*E (kPa)*	*G (kPa)*	*P (m^4/Ns)*
Chitosan	92 ± 12	5.0 ± 0.6	7.4 ± 2.0	83 ± 21	27.4 ± 21.5
CD + chitosan	–	6.4 ± 1.0	9.4 ± 1.7	71 ± 23	30.0 ± 22.9
CP + chitosan	–	7.3 ± 2.4[a]	22.0 ± 9.3[b]	143 ± 6[b]	57.6 ± 39.4
Growth plate	–	–	2239 ± 761	1249 ± 1045	1.5 ± 0.7

Chitosan, chitosan sponges kept in medium for 20 days at 37°C; CD + chitosan, chitosan sponges in culture with CD cells for 20 days; CP + chitosan, chitosan sponges in culture with CP cells for 20 days; Growth plate, growth plate of a 6-week-old chicken tibia; D, pore diameter; σ, compression strength; E, elastic modulus at 30% strain; G, aggregate modulus; P, permeability.

[a]Significantly different from chitosan sample ($p < 0.05$).

[b]Significantly different from CD + chitosan and chitosan samples ($p < 0.05$).

constructs and chitosan sponges alone had similar compression strength and permeability, while growth plate cartilage had significantly lower permeability. Chitosan sponges without cells had the lowest elastic modulus values (7.4 ± 2.0 kPa), and values for chondrocytes/chitosan constructs were different from the growth plates (2239 ± 761 kPa). Interestingly, CD chondrocytes/chitosan constructs had an elastic modulus similar to the sponge itself, while in the CP chondrocytes/chitosan constructs the elastic modulus increased approximately 2.5-fold (from 9.2 to 22 kPa). The aggregate modulus paralleled the elastic modulus.

Chondrocyte behavior on chitosan sponges

To evaluate the chondrocytes' behavior on chitosan sponges, we conducted different microscopic, histological, and biochemical analyses. Histological analyses clearly show attachment, proliferation, and extracellular matrix synthesis by

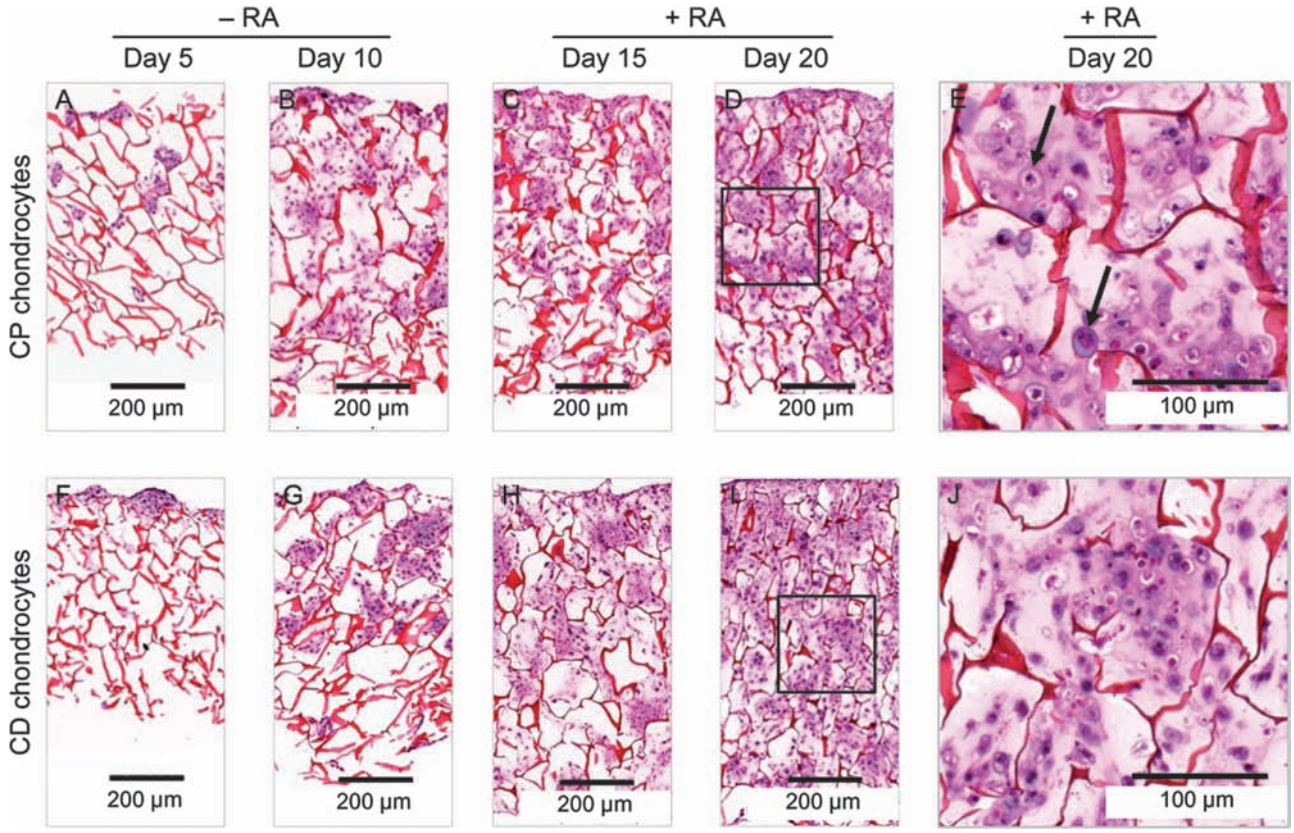

FIG. 2. Chondrocytes completely fill chitosan sponges during the culture period. Photomicrographs of H&E staining of chitosan/chondrocytes constructs cultured for 20 days. Images (**A**)–(**D**) correspond to cross sections of chitosan sponges cultured with CP chondrocytes for 5, 10, 15, and 20 days, respectively. A complete cross section of each sponge is represented in the images. Photomicrographs (**F**)–(**I**) correspond to sponges cultured with CD chondrocytes for same time points. (**E**) and (**J**) are higher magnification images of the areas inside the square in (**D**) and (**I**), respectively. Arrows in image (**E**) point to hypertrophic chondrocytes. At day 5, sponges appear thinner because during processing they did not maintain the original thickness in absence of cells/matrix. Color images available online at www.liebertonline.com/ten.

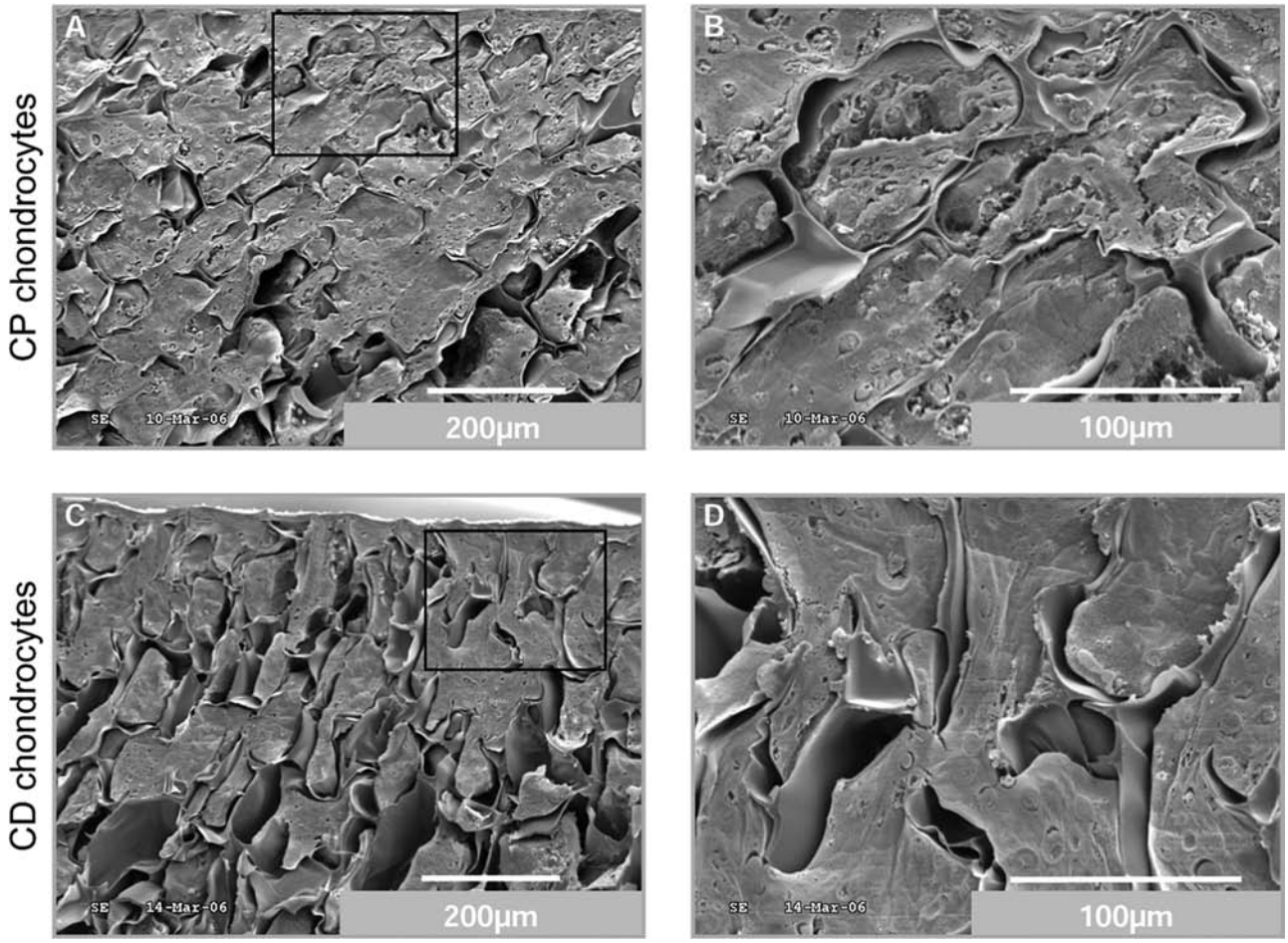

FIG. 3. An abundant matrix fills the pores of chitosan sponges. SEM analyses of cross sections of chitosan/chondrocytes constructs. At the end of the culture period, CP (**A, B**) and CD (**C, D**) chondrocytes migrated to the bottom of scaffolds and completely filled chitosan pores with a dense extra cellular matrix.

chondrocytes seeded in the chitosan sponges (Fig. 2). At day 5, cells (purple color) migrating through connecting pores can be observed for both CP and CD chondrocytes. At day 10, chondrocytes have migrated well into the depth of chitosan sponges though they do not completely fill the pores. After 15 days in culture (5 days of treatment with RA), deposition of matrix can be observed (pink material between cells). After 20 days in culture (10 days of treatment with RA), both CP and CD chondrocytes deposited an abundant extracellular matrix filling the pores of sponges. At higher magnification, hypertrophic CP chondrocytes (arrows in Fig. 2E) can be observed, while CD chondrocytes (Fig. 2J) appear smaller.

Scanning electron photomicrographs (Fig. 3) confirmed the observations from histological sections. Indeed at day 20, CP chondrocytes (Fig. 3A, B) are totally embedded in a rich extracellular matrix, completely changing the appearance of the scaffold (compare Fig. 3 with Fig. 1). The CD chondrocytes (Fig. 3C, D) also filled the pores of the chitosan sponges with a compact matrix, and no major differences can be observed between CP and CD scaffolds in these photomicrographs.

DNA measurements confirmed the increase in chondrocyte number over the culture period for both CP and CD cells. The average number of CD chondrocytes was higher than CP chondrocytes at every time point, although not statistically significant (Fig. 4). With RA treatment, the proliferation rate of CP chondrocytes decreased. At the end of the culture period, the number of CD chondrocytes was slightly higher since they maintained or even increased the proliferation rate in the presence of the retinoid.

To investigate chondrocyte maturation during the culture period, we studied two markers of hypertrophy: AP and type X collagen. In response to 10 days of RA treatment, there was a significant increase in AP activity levels in both CP and CD chondrocytes (Fig. 5). However, the levels of enzymatic activity were significantly higher in CP chondrocytes when compared to CD chondrocytes. Due to the long culture period, CD chondrocytes also responded to the retinoid; however, their AP levels after 10 days of RA exposure (7 ± 3 nmol/min/mg) were still 42-fold lower AP activity levels in CP chondrocytes exposed to RA (299 ± 109 nmol/min/mg), highlighting the different phenotypes of these cells.

Immunohistochemical analysis was conducted to detect the presence of type X collagen in the cartilage/chitosan scaffolds. As expected, in sponges seeded with CP chondrocytes, RA caused an increase in the level of type X collagen, evidenced by the strong brown color in Figure 6D. In sponges

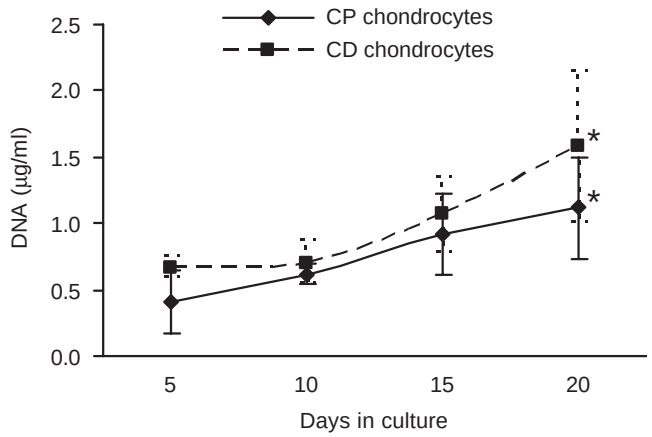

FIG. 4. Increase in DNA content of cartilage/chitosan constructs during the culture period. DNA quantification was performed in samples collected after 5, 10, 15, and 20 days in culture. Note that an increase in DNA content corresponds to an increase in chondrocytes number over the culture period for both CP and CD cells. *Significantly different from respective sample at day 5 ($p < 0.05$).

seeded with CD chondrocytes, type X collagen was not expressed at detectable levels even after 10 days of RA treatment (Fig. 6H). Counter staining with alcian blue and light green allowed visualization of proteoglycan deposition and chitosan, respectively. Although we did not quantify the staining, an intense blue color can be observed in CP chondrocytes exposed to RA for 10 days, suggesting increased proteoglycan synthesis in these samples (compare Fig. 6C with Fig. 6A, G).

To further characterize the phenotype of chondrocytes grown on the chitosan scaffold, we conducted real-time RT-PCR analysis. Results obtained are semiquantitative and presented as a "fold change" in mRNA levels in CP chondrocytes when compared to CD cells (Fig. 7). A value greater than 1, corresponds to a higher gene expression by CP chondrocytes. As expected, except for *type II collagen*, all genes studied were expressed at higher levels in CP chondrocytes than in CD chondrocytes. In response to RA treatment, *type X collagen* expression decreased (early hypertrophic marker) and *AP* gene expression increased (late hypertrophic marker). Values obtained for *runx2*, *type II collagen*, and *VEGF* are around 1; no significant differences were observed between 10 and 20 days in culture.

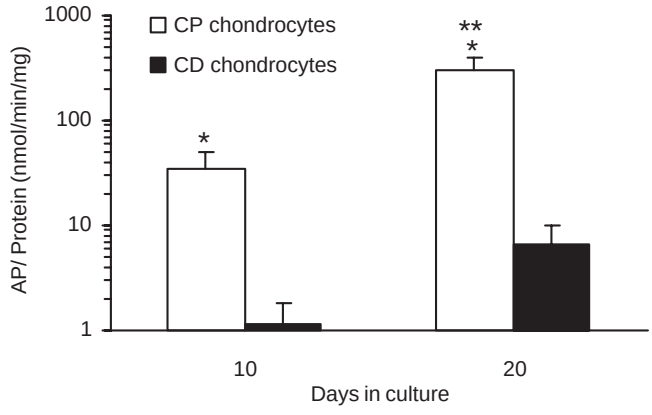

FIG. 5. RA induces AP activity in CP chondrocytes. Samples were collected after 10 and 20 days in culture. AP activity was normalized to the total protein content of each sample. The AP levels increased with time, in both CP and CD chondrocytes. *Significantly different from CD chondrocytes at same time point ($p < 0.05$). **Significantly different from same sample at day 10 ($p < 0.05$).

Discussion

Chitosan has been used as a biomaterial over the last decades and proved to be biocompatible and biodegradable.[39–41] Studies using low DA chitosan scaffolds showed that this material allows osteoblast[21,42] and articular chondrocyte[21,43] attachment and proliferation. The goal of the current study was to test the ability of this natural polymer to support proliferation and maturation of transient cartilage cells, the early steps in endochondral bone formation. The original chitosan powder from France Chitine had a DA of $\cong 30\%$, and it was deacetylated to a DA of $4.23 \pm 0.46\%$, using different temperature cycles. The deacetylation of chitosan using alkali solutions is known to lead to a decrease in both average M_w and $[\eta]$ as a result of the scission of glycosidic linkages and end-group peeling. Chitosan with a DA of 4% was previously reported to enable the attachment and proliferation of both osteoblasts and rat bone marrow stromal cells.[33] Therefore, chitosan with this DA was selected to produce sponges. The 3D homogeneous structures prepared presented highly interconnected pores of average size shown to allow robust chondrocyte proliferation and metabolic activity.[44] RA was used to induce chondrocyte maturation into hypertrophic cells. RA is one of the more biologically active derivatives of retinol (vitamin A) and a well-known regulator of cartilage and skeletal formation.[45–47] We cultured both cells representative of a transient cartilage phenotype, CP chondrocytes, and cells that maintain a more stable phenotype, CD chondrocytes. CD cells do not readily undergo hypertrophy in response to RA and therefore were used as a "permanent" cartilage control.

In 10 days, both CP and CD chondrocytes migrated into pores deep in the chitosan sponges completely obliterating some spaces, attesting to the excellent interconnectivity between the pores. Cell proliferation continued for both CD and CP chondrocytes even during treatment with RA, though CP cells showed a slight decrease after day 15. According to Gentili *et al.*,[48] chondrocyte proliferation stops only after mineralization has been started. However, in our studies we did not supplement the media with β-glycerophosphate or another phosphate source. Thus, our chondrocytes, while expressing high AP levels, did not deposit mineral (microcomputerized tomography results not shown).

Cells proliferation and matrix deposition increased in both CD and CP chondrocyte–seeded scaffolds over the culture period. It was expected that the abundant matrix synthesis would drastically change the mechanical properties of the chitosan sponges. However, while elastic modulus, a measure of stiffness, increased threefold for chitosan sponges seeded with CP chondrocytes, it did not change significantly for chitosan sponges seeded with CD chondrocytes. Therefore, more than the quantity, it was the quality of the matrix deposited that mostly affected stiffness of chondrocyte/chitosan

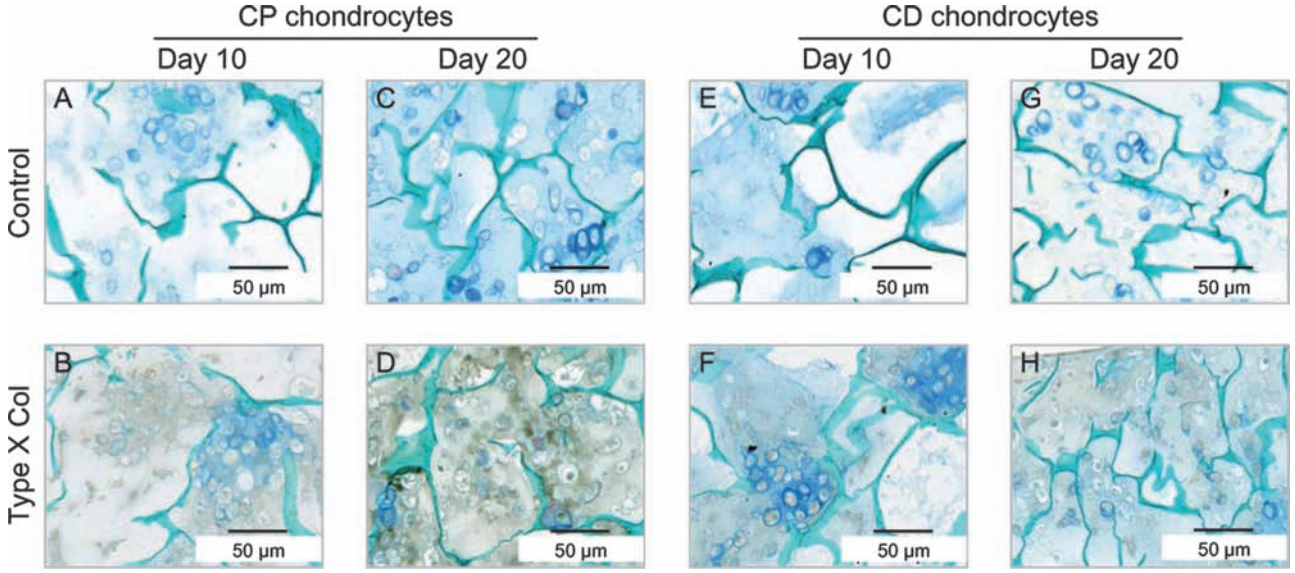

FIG. 6. RA increases type X collagen in scaffolds seeded with CP chondrocytes. Immunohistochemical analyses of type X collagen was performed on deparaffinized sections of CP (**A–D**) and CD (**E–H**) chondrocytes. Sections were counterstained with alcian blue to visualize proteoglycans and light green to label the chitosan walls. Photomicrographs (**A**), (**B**), (**E**), and **(F)** correspond to 10 days in culture, and pictures (**C**), (**D**), (**G**), and (**H**) correspond to 20 days in culture. Upper panels show controls (incubated with preimmune serum) of respective bottom panels. Color images are available online at www .liebertonline.com/ten.

constructs. Indeed, type X collagen has been reported to increase the matrix stiffness by Naumann *et al*.[49] The stiffness of CP chondrocytes/chitosan constructs is 100-fold lower than the stiffness of chicken growth plates. Since ceramic phases present higher compression strength than unmineralized tissues, we believe that we would observe different mechanical properties had the cultured chondrocytes been allowed to mineralize the extracellular matrix as it occurs in the native growth plate.

Although both CP and CD chondrocytes responded to RA by increasing matrix deposition, the nature of this matrix was found to be dependent on the type of cell. CP cells responded to the retinoid by expressing the hypertrophic phenotype, characterized by the presence of type X collagen in their matrix and increased AP activity. Indeed, all regulators or markers of hypertrophy studied (*runx2*, *VEGF*, *type X collagen*, and *AP*) were expressed at higher levels in the CP cells when compared to the CD chondrocytes, supporting the different phenotype of these cell populations. However, overtime we observed a decrease in *type X collagen* expression and an increase in *AP* expression in CP cells. These results agree with *in vivo* data showing that *type X collagen* expression occurs in early hypertrophic chondrocytes while *AP*, a later maturation marker involved in matrix mineralization, is expressed by terminally differentiated chondrocytes in the calcified region of the growth plate.[50–52]

Several studies have demonstrated that chitosan supports the articular chondrocyte phenotype and activity. The study of Lu *et al*.[23] showed that chitosan injected into the knee articular cavity of rats caused a significant increase in the density of chondrocytes in the knee articular cartilage. Also, abundant cartilage extracellular matrix protein[43] was obtained after injecting nude mice subcutaneously with an *in situ*–gelling chitosan solution cultured with chondrocytes. Further, when pig chondrocytes were cultured on porous chitosan scaffolds, they were able to proliferate and to spread into the sponges, with larger interconnected pores improving the cellularity and matrix content.[44] Another study revealed that primary chondrocytes cultured on chondroitin 4-sulfate/chitosan maintained the synthesis of cartilage-specific collagens.[17] Similar results were achieved using chitosan films seeded

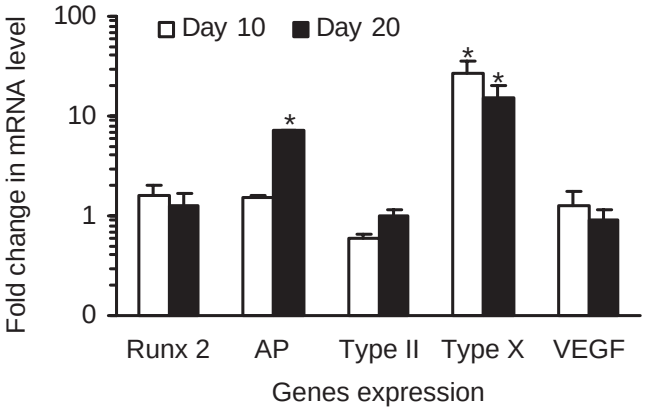

FIG. 7. Gene expression profile of CP chondrocytes cultured in chitosan sponges. Real-time RT-PCR semiquantitative results are presented as fold change in mRNA levels of CP chondrocytes when compared to CD cells. Samples with CP and CD chondrocytes were both analyzed, and a fold change higher than 1 corresponds to a higher gene expression by CP chondrocytes. *Significantly different from CD chondrocytes at same time point ($p < 0.05$).

with both human osteoblasts and chondrocytes.[21] Osteoblasts were able to spread and to express *collagen type I*, whereas chondrocytes expressed *collagen type II*, suggesting that a chitosan scaffold is able to maintain both cells original phenotype.

Amaral *et al*.[53] investigated human osteoblast behavior in chitosan scaffolds similar to those used in the present study. They found that osteoblasts attach well and spread on chitosan sponges, displaying long cell filopodia and numerous cell–cell contacts. A major limitation in tissue engineering has been the availability of nutrients and oxygen once the construct reaches a critical mass. And in that aspect, osteoblasts are particularly susceptible.[54–57] Cartilage (growth plate and articular cartilage), however, is characterized by large avascular regions and excellent adaptation to hypoxic conditions.[58,59] In fact, evidence supports the role of low oxygen levels in chondrocyte differentiation and endochondral bone formation.[60] These properties provide support to the bone tissue engineering approach here investigated, which explores the endochondral ossification pathway for the correction of extensive bone defects.

All the studies mentioned earlier used chitosan as a scaffold for either articular cartilage or bone. Here we reported the use of chitosan sponges as a template for transient cartilage and the creation of an improved osteoinductive scaffold for bone regeneration. Indeed, hypertrophic chondrocytes secrete factors capable of inducing osteoblast and osteoclast activity, as well as vascularization.[28,61–64] All these different cell types and their activity are necessary and responsible for endochondral bone formation. Indeed, parallel studies conducted in our laboratory show the ability of this transient cartilage/chitosan constructs to induce endochondral bone formation in the subcutaneous region of nude mice (see accompanying article).[65]

Conclusions

The use of osteoblasts or osteoprogenitor cells to promote bone regeneration is the method most commonly exploited in current tissue engineering approaches. However, nature mostly uses the endochondral ossification pathway during bone formation, growth, and healing after fracture. In addition to these considerations, there are numerous other advantages to explore the endochondral pathway for bone tissue engineering. Chondrocytes are resistant to low oxygen levels and can induce vascular invasion and osteogenesis. In this study, chitosan sponges served as excellent support for chondrocyte proliferation and intense matrix deposition. As a result of the activity of the transient cartilage cells, the mechanical properties of the chitosan scaffold changed drastically and favorably. These scaffolds can now be used as osteoinductive grafts *in vivo*, inducing and remodeling into bone, mimicking the natural process of endochondral ossification.

Acknowledgments

This work was supported by the Luso-American Development Foundation (Portugal), the Calouste Gulbenkian Foundation (Portugal), PRODEP (Portugal), and the American Association of Orthodontics Foundation and by NIDCR Grant 5K08DE017426. The authors thank Ms. Gloria Turner, Department of Pathology at New York University College of Dentistry, for her important assistance in preparation of samples for histology and immunohistochemistry. Mechanical tests were performed at the NIH-sponsored Musculoskeletal Repair and Regeneration Core Center at the Hospital for Special Surgery (AR046121).

References

1. Steinemann, S.G. Metal implants and surface reactions. Injury **27,** 16, 1996.
2. Disegi, J.A., and Eschbach, L. Stainless steel in bone surgery. Injury **31,** 2, 2000.
3. Reitman, R.D., Emerson, R., Higgins, L., and Head, W. Thirteen year results of total hip arthroplasty using a tapered titanium femoral component inserted without cement in patients with type C bone. J Arthroplasty **18,** 116, 2003.
4. Epinette, J.A., Manley, M.T., D'Antonio, J.A., Edidin, A.A., and Capello, W.N. A 10-year minimum follow-up of hydroxyapatite-coated threaded cups: clinical, radiographic and survivorship analyses with comparison to the literature. J Arthroplasty **18,** 140, 2003.
5. Xynos, I.D., Hukkanen, M.V., Batten, J.J., Buttery, L.D., Hench, L.L., and Polak, J.M. Bioglass 45S5 stimulates osteoblast turnover and enhances bone formation *in vitro*: implications and applications for bone tissue engineering. Calcif Tissue Int **67,** 321, 2000.
6. Barrias, C.C., Ribeiro, C.C., and Barbosa, M.A. Adhesion and proliferation of human osteoblastic cells seeded on injectable hydroxyapatite microspheres. Bioceramics **254,** 877, 2004.
7. Saito, N., and Takaoka, K. New synthetic biodegradable polymers as BMP carriers for bone tissue engineering. Biomaterials **24,** 2287, 2003.
8. Suzuki, T., Kawamura, H., Kasahara, T., and Nagasaka, H. Resorbable poly-L-lactide plates and screws for the treatment of mandibular condylar process fractures: a clinical and radiologic follow-up study. J Oral Maxillofac Surg **62,** 919, 2004.
9. Sittinger, M., Reitzel, D., Dauner, M., Hierlemann, H., Hammer, C., Kastenbauer, E., Planck, H., Burmester, G.R., and Bujia, J. Resorbable polyesters in cartilage engineering: affinity and biocompatibility of polymer fiber structures to chondrocytes. J Biomed Mater Res **33,** 57, 1996.
10. Vaccaro, A.R., Singh, K., Haid, R., Kitchel, S., Wuisman, P., Taylor, W., Branch, C., and Garfin, S. The use of bioabsorbable implants in the spine. Spine J **3,** 227, 2003.
11. Jianqi, H., Hong, H., Lieping, S., and Genghua, G. Comparison of calcium alginate film with collagen membrane for guided bone regeneration in mandibular defects in rabbits. J Oral Maxillofac Surg **60,** 1449, 2002.
12. Chan, C., Thompson, I., Robinson, P., Wilson, J., and Hench, L. Evaluation of bioglass/dextran composite as a bone graft substitute. Int J Oral Maxillofac Surg **31,** 73, 2002.
13. Mukherjee, D.P., Tunkle, A.S., Roberts, R.A., Clavenna, A., Rogers, S., and Smith, D. An animal evaluation of a paste of chitosan glutamate and hydroxyapatite as a synthetic bone graft material. J Biomed Mater Res B Appl Biomater **67B,** 603, 2003.
14. Sashiwa, H., and Aiba, S. Chemically modified chitin and chitosan as biomaterials. Prog Polym Sci **89,** 887, 2004.
15. Hoekstra, A., Struszczyk, H., and Kivekas, O. Percutaneous microcrystalline chitosan application for sealing arterial puncture sites. Biomaterials **19,** 1467, 1998.
16. Lee, K.Y., Ha, W.S., and Park, W.H. Blood compatibility and biodegradability of partially N-acylated chitosan derivatives. Biomaterials **16,** 1211, 1995.

17. Suh, J.K., and Matthew, H.W. Application of chitosan-based polysaccharide biomaterials in cartilage tissue engineering: a review. Biomaterials **21,** 2589, 2000.
18. Hirano, S., Tsuchida, H., and Nagao, N. N-acetylation in chitosan and the rate of its enzymic hydrolysis. Biomaterials **10,** 574, 1989.
19. Prashanth, K.V.H., and Tharanathan, R.N. Chitin/chitosan: modifications and their unlimited application potential—an overview. Trends Food Sci Technol **18,** 117, 2007.
20. Chellat, F., Tabrizian, M., Dumitriu, S., Chornet, E., Hilaire, C., and Yahia, R. Study of biodegradation behavior of chitosan-xanthan microspheres in simulated physiological media. J Biomed Mater Res **53,** 592, 2000.
21. Lahiji, A., Sohrabi, A., Hungerford, D.S., and Frondoza, C.G. Chitosan supports the expression of extracellular matrix proteins in human osteoblasts and chondrocytes. J Biomed Mater Res **51,** 586, 2000.
22. Nettles, D.L., Elder, S.H., and Gilbert, J.A. Potential use of chitosan as a cell scaffold material for cartilage tissue engineering. Tissue Eng **8,** 1009, 2002.
23. Lu, J.X., Prudhommeaux, F., Meunier, A., Sedel, L., and Guillemin, G. Effects of chitosan on rat knee cartilages. Biomaterials **20,** 1937, 1999.
24. Abe, M., Takahashi, M., Tokura, S., Tamura, H., and Nagano, A. Cartilage-scaffold composites produced by bioresorbable beta-chitin sponge with cultured rabbit chondrocytes. Tissue Eng **10,** 585, 2004.
25. Sechriest, V.F., Miao, Y.J., Niyibizi, C., Westerhausen-Larson, A., Matthew, H.W., Evans, C.H., Fu, F.H., and Suh, J.K. GAG-augmented polysaccharide hydrogel: a novel biocompatible and biodegradable material to support chondrogenesis. J Biomed Mater Res **49,** 534, 2000.
26. Rajpurohit, R., Koch, C.J., Tao, Z., Teixeira, C.M., and Shapiro, I.M. Adaptation of chondrocytes to low oxygen tension: relationship between hypoxia and cellular metabolism. J Cell Physiol **168,** 424, 1996.
27. Maes, C., Carmeliet, P., Moermans, K., Stockmans, I., Smets, N., Collen, D., Bouillon, R., and Carmeliet, G. Impaired angiogenesis and endochondral bone formation in mice lacking the vascular endothelial growth factor isoforms VEGF164 and VEGF188. Mech Dev **111,** 61, 2002.
28. Petersen, W., Tsokos, M., and Pufe, T. Expression of VEGF121 and VEGF165 in hypertrophic chondrocytes of the human growth plate and epiphyseal cartilage. J Anat **201,** 153, 2002.
29. Pullig, O., Weseloh, G., Ronneberger, D., Kakonen, S., and Swoboda, B. Chondrocyte differentiation in human osteoarthritis: expression of osteocalcin in normal and osteoarthritic cartilage and bone. Calcif Tissue Int **67,** 230, 2000.
30. Hashimoto, S., Ochs, R.L., Rosen, F., Quach, J., McCabe, G., Solan, J., Seegmiller, J.E., Terkeltaub, R., and Lotz, M. Chondrocyte-derived apoptotic bodies and calcification of articular cartilage. Proc Natl Acad Sci USA **95,** 3094, 1998.
31. Pullig, O., Weseloh, G., Gauer, S., and Swoboda, B. Osteopontin is expressed by adult human osteoarthritic chondrocytes: protein and mRNA analysis of normal and osteoarthritic cartilage. Matrix Biol **19,** 245, 2000.
32. Eerola, I., Salminen, H., Lammi, P., Lammi, M., von der Mark, K., Vuorio, E., and Saamanen, A.M. Type X collagen, a natural component of mouse articular cartilage: association with growth, aging, and osteoarthritis. Arthritis Rheum **41,** 1287, 1998.
33. Amaral, I.F., Sampaio, P., and Barbosa, M.A. Three-dimensional culture of human osteoblastic cells in chitosan sponges: the effect of the degree of acetylation. J Biomed Mater Res A **76,** 335, 2006.
34. Mow, V.C., Kuei, S.C., Lai, W.M., and Armstrong, C.G. Biphasic creep and stress relaxation of articular cartilage in compression? Theory and experiments. J Biomech Eng **102,** 73, 1980.
35. Iwamoto, M., Shapiro, I.M., Yagami, K., Boskey, A.L., Leboy, P.S., Adams, S.L., and Pacifici, M. Retinoic acid induces rapid mineralization and expression of mineralization-related genes in chondrocytes. Exp Cell Res **207,** 413, 1993.
36. Teixeira, C.C., Hatori, M., Leboy, P.S., Pacifici, M., and Shapiro, I.M. A rapid and ultrasensitive method for measurement of DNA, calcium and protein content, and alkaline phosphatase activity of chondrocyte cultures. Calcif Tissue Int **56,** 252, 1995.
37. Nehrer, S., Breinan, H.A., Ramappa, A., Young, G., Shortkroff, S., Louie, L.K., Sledge, C.B., Yannas, I.V., and Spector, M. Matrix collagen type and pore size influence behaviour of seeded canine chondrocytes. Biomaterials **18,** 769, 1997.
38. Karande, T.S., Ong, J.L., and Agrawal, C.M. Diffusion in musculoskeletal tissue engineering scaffolds: design issues related to porosity, permeability, architecture, and nutrient mixing. Ann Biomed Eng **32,** 1728, 2004.
39. VandeVord, P.J., Matthew, H.W., DeSilva, S.P., Mayton, L., Wu, B., and Wooley, P.H. Evaluation of the biocompatibility of a chitosan scaffold in mice. J Biomed Mater Res **59**, 585, 2002.
40. Hong, Y., Song, H., Gong, Y., Mao, Z., Gao, C., and Shen, J. Covalently crosslinked chitosan hydrogel: Properties of *in vitro* degradation and chondrocyte encapsulation. Acta Biomater **3,** 23, 2007.
41. Ho, M., Wang, D., Hsieh, H., Liu, H.C., Hsien, T.Y., Lai, J.Y., and Hou, L.T. Preparation and characterization of RGD-immobilized chitosan scaffolds. Biomaterials **26,** 3197, 2005.
42. Amaral, I.F., Cordeiro, A.L., Sampaio, P., and Barbosa, M.A. Attachment, spreading and short-term proliferation of human osteoblastic cells cultured on chitosan films with different degrees of acetylation. J Biomater Sci Polym Ed **18,** 469, 2007.
43. Hoemann, C.D., Sun, J., Legare, A., McKee, M.D., and Buschmann, M.D. Tissue engineering of cartilage using an injectable and adhesive chitosan-based cell-delivery vehicle. Osteoarthritis Cartilage **13,** 318, 2005.
44. Griffon, D.J., Sedighi, M.R., Schaeffer, D.V., Eurell, J.A., and Johnson, A.L. Chitosan scaffolds: interconnective pore size and cartilage engineering. Acta Biomater **2,** 313, 2006.
45. Underhill, T.M., and Weston, A.D. Retinoids and their receptors in skeletal development. Microsc Res Tech **43,** 137, 1998.
46. Cohen, A.J., Lassova, L., Golden, E.B., Niu, Z., and Adams, S.L. Retinoids directly activate the collagen X promoter in prehypertrophic chondrocytes through a distal retinoic acid response element. J Cell Biochem **99,** 269, 2006.
47. Pacifici, M., Golden, E.B., Iwamoto, M., and Adams, S.L. Retinoic acid treatment induces type X collagen gene expression in cultured chick chondrocytes. Exp Cell Res **195,** 38, 1991.
48. Gentili, C., Bianco, P., Neri, M., Malpeli, M., Campanile, G., Castagnola, P., Cancedda, R., and Cancedda, F.D. Cell-proliferation, extracellular-matrix mineralization, and ovotransferrin transient expression during in-vitro differentiation of chick hypertrophic chondrocytes into osteoblast-like cells. J Cell Biol **122,** 703, 1993.

49. Naumann, A., Dennis, J.E., Awadallah, A., Carrino, D.A., Mansour, J.M., Kastenbauer, E., and Caplan, A.I. Immunochemical and mechanical characterization of cartilage subtypes in rabbit. J Histochem Cytochem **50,** 1049, 2002.
50. Wang, W., and Kirsch, T. Retinoic acid stimulates annexin-mediated growth plate chondrocyte mineralization. J Cell Biol **157,** 1061, 2002.
51. Whyte, M.P. Hypophosphatasia and the role of alkaline phosphatase in skeletal mineralization. Endocr Rev **15,** 439, 1994.
52. Lewinson, D., Toister, Z., and Silbermann, M. Quantitative and distributional changes in the activity of alkaline phosphatase during the maturation of cartilage. J Histochem Cytochem **30,** 261, 1982.
53. Amaral, I.F., Sampaio, P., and Barbosa, M.A. Three-dimensional culture of human osteoblastic cells in chitosan sponges: the effect of the degree of acetylation. J Biomed Mater Res A **76,** 335, 2005.
54. Park, J.H., Park, B.H., Kim, H.K., Park, T.S., and Baek, H.S. Hypoxia decreases Runx2/Cbfa1 expression in human osteoblast-like cells. Mol Cell Endocrinol **192,** 197, 2002.
55. Utting, J.C., Robins, S.P., Brandao-Burch, A., Orriss, I.R., Behar, J., and Arnett, T.R. Hypoxia inhibits the growth, differentiation and bone-forming capacity of rat osteoblasts. Exp Cell Res **312,** 1693, 2006.
56. Warren, S.M., Steinbrech, D.S., Mehrara, B.J., Saadeh, P.B., Greenwald, J.A., Spector, J.A., Bouletreau, P.J., and Longaker, M.T. Hypoxia regulates osteoblast gene expression. J Surg Res **99,** 147, 2001.
57. Salim, A., Nacamuli, R.P., Morgan, E.F., Giaccia, A.J., and Longaker, M.T. Transient changes in oxygen tension inhibit osteogenic differentiation and Runx2 expression in osteoblasts. J Biol Chem **279,** 40007, 2004.
58. Vu, T.H., Shipley, J.M., Bergers, G., Berger, J.E., Helms, J.A., Hanahan, D., Shapiro, S.D., Senior, R.M., and Werb, Z. MMP-9/gelatinase B is a key regulator of growth plate angiogenesis and apoptosis of hypertrophic chondrocytes. Cell **93,** 411, 1998.
59. Skawina, A., Litwin, J.A., Gorczyca, J., and Miodonski, A.J. The vascular system of human fetal long bones: a scanning electron microscope study of corrosion casts. J Anat **185,** 369, 1994.
60. Pfander, D., Cramer, T., Schipani, E., and Johnson, R.S. HIF-1alpha controls extracellular matrix synthesis by epiphyseal chondrocytes. J Cell Sci **116,** 1819, 2003.
61. Deckers, M.M., Karperien, M., van der Bent, C., Yamashita, T., Papapoulos, S.E., and Lowik, C.W. Expression of vascular endothelial growth factors and their receptors during osteoblast differentiation. Endocrinology **141,** 1667, 2000.
62. Gerber, H.P., Vu, T.H., Ryan, A.M., Kowalski, J., Werb, Z., and Ferrara, N. VEGF couples hypertrophic cartilage remodeling, ossification and angiogenesis during endochondral bone formation. Nat Med **5,** 623, 1999.
63. Nakagawa, M., Kaneda, T., Arakawa, T., Morita, S., Sato, T., Yomada, T., Hanada, K., Kumegawa, M., and Hakeda, Y. Vascular endothelial growth factor (VEGF) directly enhances osteoclastic bone resorption and survival of mature osteoclasts. FEBS Lett **473,** 161, 2000.
64. Pfander, D., Kortje, D., Zimmermann, R., Weseloh, G., Kirsch, T., Gesslein, M., Cramer, T., and Swoboda, B. Vascular endothelial growth factor in articular cartilage of healthy and osteoarthritic human knee joints. Ann Rheum Dis **60,** 1070, 2001.
65. Oliveira, S.M., Turner, G., Mijares, D., Amaral, I.F., Barbosa, M.A., and Teixeira, C.C. Engineering endochondral bone: *in vivo* studies. 2007.

Address reprint requests to:
Cristina C. Teixeira, D.M.D., M.S., Ph.D.
Departments of Basic Science and Craniofacial Biology and of Orthodontics
New York University College of Dentistry
345 East 24th St.
New York, NY 10010

E-mail: ct40@nyu.edu

Received: January 23, 2008
Accepted: June 6, 2008
Online Publication Date: August 28, 2008